

J.F. Jamet and M.H. Ritti

Office National d'Etudes et de Recherches Aérospatiales
BP. 72, 92322 CHATILLON, FranceAbstract

ONERA has recently developed a general process based on the infiltration of ultrafine ceramic powders in ceramic fibers multi-D preforms which is based on the pressure slip casting technique.

Currently, alumina reinforced by SiC Nicalon fibers gives promising mechanical results with uni-directional (350 MPa) and tridirectional reinforcements (250 MPa). Mechanical behaviour (critical strengths, maximal strengths and toughness) are directly related to the number of infiltrations and to the ultimate sintering treatments. This high yield densification processing, which requires no pressure during sintering, gives the opportunity of :

- treating a wide range of preforms and large structures ;
- meeting uniform composite microstructure ;
- introducing gel or organometallic precursors with the advantage of both techniques.

1. Introduction

Fiber-reinforced ceramic matrix composites are a promising class of structural materials for aerospace applications where high strength, high toughness, low thermal expansion, low density and high temperature stability are desirable attributes. Though science and technology have made great steps in recent years in this area, the key of the realization of large ceramic composites structures for aerospace applications which requires greatly improved reliability, and better thermomechanical properties is the development of improved methods of processing.

Among the four categories of processing methods (slurry infiltration technique, chemical synthesis route, melt infiltration and chemical vapor infiltration), the CVI method is presently the only one to be credible for large structures (SEP work in France). As a matter of fact, this method produces excellent quality matrices (Ex : SiC) inside large and thin fiber preforms under vacuum furnace and the only limitations are the dimensions of the vacuum furnace. The melt infiltration method is limited by hot press techniques. The chemical synthesis route using sol-gel or polymers pyrolysis could be a promising method because the infiltration of such precursors is very easy, nevertheless the main drawbacks are the high shrinkage and the low yield, which precludes the formation of a dense matrix without further processing steps. Slurry infiltration is certainly the most common technique to produce ceramic matrix composites in which a tow or fabric is impregnated by passage through a slurry mixture containing the matrix material. The dried impregnated system is then cut into desired configurations and hot pressed. This technique has presently been used most effectively with glass and

glass ceramic matrix composites which are typically hot pressed at temperatures near or above the softening point of the glass (Ex : UTRC materials). With the same nature of matrix, pressure-assisted melt-infiltration is still possible.

Meanwhile, slurry processing applied to refractory crystalline matrix systems has been less effective because of the absence of viscous flow and their higher temperature required to densify the matrices. This is why ONERA started two years ago a research program to develop a high yield depth-infiltration processing of very fine crystalline powders extensible to high fiber content 3D preforms. This program leans on the carbon-carbon experience and on promising results obtained with the combined slurry-gel (or polymer precursor) approach, with the advantages of both techniques (1).

This paper relates this extension of the slurry infiltration which was mainly investigated using the pressure slip casting technique based on ultrafine crystalline α -alumina powders. It describes the possibilities of the technique with one-, two- or three-dimensional fiber preforms using mainly SiC Nicalon and alumina FP and gives the mechanical behaviour of these free sintered systems and prospects of the process.

2. Colloidal filtration

Several authors, in recent years (2,3,4) have shown through colloidal filtration mechanics studies, that it was possible to obtain very homogeneous compacts of high green density by using a fine, narrow size distribution powder, dispersed to form a stable colloidal suspension by appropriate control of the particle surface charge. The casting rate has been shown to be proportional to the pressure differential across the filter (5). The pressure slip casting technique is the appropriate tool to develop such colloidal filtration. Fig. 1 presents the diagram of the basic filtration apparatus. It includes two main volumes separated by a special filter against which very fine powder ($0.1 \mu\text{m} < d < 1 \mu\text{m}$) is stopped and through which the carrier liquid is evacuated. In the upper volume, the slurry is introduced and the pressure is controlled, up to 1 MPa. In the lower volume, the evacuated liquid is collected and its volume measured ; the pressure is controlled by a vacuum system.

For the present study which involves the colloid transport through a fiber preform, an intermediate chamber was added. The latter is located immediately above the filter and the fibers volume ratio is controlled by the position of the upper grid. Such an apparatus allowed basic investigations on liquid and colloidal filtrations of many slurry systems (fine powder + liquid carrier) with or without various fiber preforms.

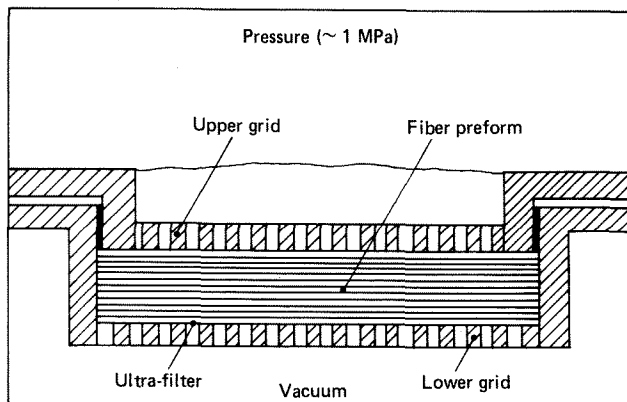


Figure 1. Pressure slip casting system

2.1. Transport and deposition mechanisms

The new problem which has to be solved for this process concerns the deposition of particles through the fiber preform which involves the best condition of transport and the non-attachment of particles on the fibers surface. The attachment mechanism is governed by the same forces which are important in flocculation (electrical and van der Waals). These are of rather short range, whereas particles need to be transported over comparatively large distances from the bulk suspension to the fibers surface. For this reason, it is usually justified to treat the transport and attachment steps separately.

Three main transport mechanisms are regarded as important in the filtration of liquid suspensions through porous media. These are convective diffusion, interception and sedimentation. Theories have been developed which enable the capture efficiency of a collector to be calculated for each of the transport mechanisms (7). The essential qualitative features of the results are summarized in table 1.

Decreasing of capture by	Particles		Collector size	Flow rate
	Size	Density		
Convective diffusion	↗	→	↗	↗
Interception	↘	→	↗	→
Sedimentation	↘	→	↗	↘

Table 1 - Capture efficiency of a collector relative to the main transport mechanisms in liquid suspensions

Because small particles are captured more effectively by diffusion and large particles by interception and sedimentation, there should be a certain particle size at which capture efficiency is minimal. This condition is requested in the present application to allow the transport of particles through the fiber preform up to the filter and to obtain the maximum cake density in the porous medium. It occurs for particles around 1 μm in diameter (8).

Now, to avoid attachment (for the same reason), the particle-fiber interaction needs to be favorable, which means essentially repulsion between them. If this condition is not met, some form of pre-treatment will be necessary, for instance by increasing the charge on particles or fiber preform or both.

So, after an initial period of particles transport through the fiber preform, the medium quickly becomes blocked and particles are removed entirely by straining through a layer of filtered particles using gas pressure. At this point, such a cake filtration is widely used in the separation of solids from relatively concentrated suspensions such as described by previous references: Svarovsky (2) and Ashkay (3,4,5).

Let us emphasize that the conditions for cake filtration are not inconsistent with those previous required by particle transport through the fiber preform.

2.2. Alumina transport and deposition in fiber preform

The present description concerns the transport and deposition of very fine α -alumina powders (Sumitomo and Bałkowski) in 1D, 2D and 3D fiber preforms (FP alumina and SiC Nicalon fibers). Components properties are presented in table 2 and 3.

	Sumitomo AKP 50	Bałkowski 6749
Purity	99.99 %	99.99 %
Phase α	(90 %)	(80-85 %)
Mean size (μm)	0.25	0.35
Specific area (m^2/g)	12	7.8
2000 psi density	1.98	1.89

Table 2 - Alumina powders specifications

Parameters	SiC Nicalon	Alumina FP
σ_{fu} (MPa)	2060	1900
E_f (GPa)	206	380
ϵ_{fu}	$10 \cdot 10^{-3}$	$4.5 \cdot 10^{-3}$
α_f ($^{\circ}\text{C}^{-1}$)	$3 \cdot 10^{-6}$	$8.7 \cdot 10^{-6}$
ϕ_f (μm)	12	20

Table 3 - SiC Nicalon and Alumina FP fibers specifications

We have previously indicated that the first condition requested for particle transport in a large size collector occurs with particle around 1 μm in diameter. The grade of Sumitomo and Bałkowski alumina powders chosen here is simultaneously consistent with this condition and with the large size collector condition ($35 < \text{fiber/particle diameters ration} < 80$).

The second condition for particle transport requires the stability of the discrete particle hydrosol. This condition, which depends on the size and concentration of particles, the nature of particle surface and the composition of the solution, was realized in deionized water at a concentration of 50 % by weight. The pH of the solution was adjusted to 3-4 and the particles dispersed using an ultrasonic bath.

This hydrosol composition and pressure slip casting conditions were optimized to reach the maximum alumina green plate density (without fiber preform). So, the entire casting vessel is evacuated before the hydrosol is introduced into the mold, then the upper chamber is pressurized to 0.6-1 MPa with argon gas, and casting continues until water ceased to accumulate in the evacuated lower chamber (30 mn). Alumina green plates are produced approximately 10 mm thick, 65 mm long, by 40 mm wide. After drying, such an optimized processing gives green plates which present a relatively high bulk density which is 2370 kg/m^3 with Sumitomo AKP 50 powder and 2390 kg/m^3 with Bałkowski 6749 powder. Such alumina bulk densities correspond to around 40 % porosity.

The efficiency of transport and deposition in 1D, 2D and 3D fiber preforms was investigated with this last optimized pressure slip casting processing. Nevertheless, the last condition to avoid particle attachment required electric repulsion charges between particles and fibers. Such a condition was easily met with FP alumina fiber because the nature of surface powder was the same. On the SiC Nicalon fiber, a heat treatment in air (500°C during 90 mn) oxidizes the surface, creates Si-O bounds on which hydroxyl groups are rapidly established. Such a modified surface is then easily charged by an electrolyte pre-filtration (pH 3 water).

Four different fibers preforms were investigated under this processing; table 4 presents these preforms specifications, composites and matrices green bulk densities and their deposition yields (relative to unreinforced plate green density). Results obtained with the two alumina powders are so closed, only Bałkowski results are mentioned here.

Fibers	Fibers di- rec- tion	Pre- form thick- ness (mm)	Fiber volume			Compo- site G.B.D. (* (*))	Matrix G.B.D. (* (*))	Depo- sition yield (%)
			X	Y	Z			
Alumi- na FP	1D	4	.37	--	--	2.72	2.00	84
SiC	1D	4	.23	--	--	2.30	2.27	95
Nica- lon	2D	1	.17	.18	--	2.38	2.30	97
	3D	8	.19	.19	.06	2.35	2.26	95

Table 4 - Alumina deposition efficiencies into various ceramic fiber preforms

These results show the efficiency of such a process which allows to deposit directly and homogeneously α -alumina into a 8 mm thick 3D SiC preform ($V_f = 45\%$) with a green density close to 2300 kg/m^3 , i.e. a bulk porosity of the composite before sintering of only 23 %. The lower deposition yield obtained with FP alumina (84 %) is mainly explained by the surface roughness of the fibers.

At this point, two processing routes could be followed :

- 1) Direct free sintering of the infiltrated fiber preform ;
- 2) Extension of the densification by alumina sol-gel infiltrations.

The second route, which improved considerably the densification efficiency, put forward the problem of the reactivity with the fibers, which can be solved by an anti-adhesion pre-treatment of the latter (coating technique). This process which is being presently developed at ONERA is beyond the scope of this paper.

3. SINTERING STAGE AND MECHANICAL BEHAVIOUR

3.1. Non-reinforced alumina

The very low size of the alumina particles and the relatively high density of the green matrix obtained by this process reduce simultaneously the sintering temperature and the shrinkage of the matrix. Figure 2 shows the evolutions of density and shrinkage of this non-reinforced matrix versus sintering temperature (duration : 30 mn). Ultimate free sintering is reached at 1400°C and the corresponding shrinkage is only 15 %.

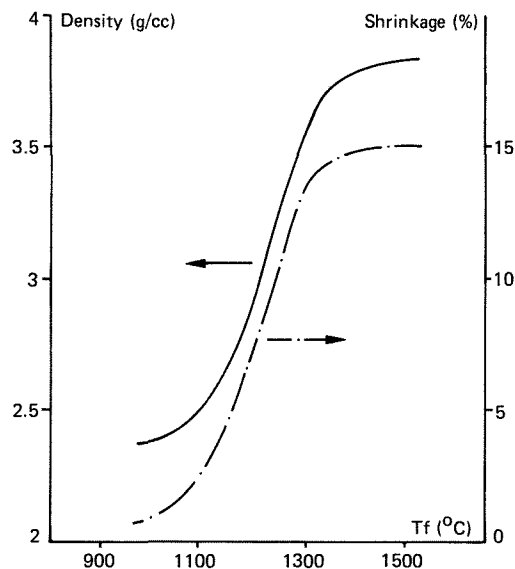


Figure 2. Unreinforced alumina matrix density and shrinkage evolution during free sintering

* Green Bulk Density

In order to allow a comparison of the mechanical behaviour of these composites with models, the pertinent structural and mechanical parameters were determined for the matrix as a function of the sintering temperature. Table 5 gives the experimental results obtained at 1200, 1275 and 1400°C using Vickers indentation and the single edged notched beam technique.

Sintering T °C	ρ_m g/cc	Pm %	Hv _m GPa	Em GPa	Klc MPa \sqrt{m}	σ_m MPa
1200	2,9	27	8,8	113	1,4	93
1275	3,5	14	17,7	229	2,9	185
1400	3,8	3,8	30,2	388	4,9	318

Table 5 - Mechanical properties of the unreinforced α -alumina as a function of the sintering temperature

The fitted expressions of Young modulus, Klc and ultimate strength, as a function of the porosity are the following :

$$E_m = 475 \exp(-5,3 P) \quad (\text{GPa})$$

$$Klc = 6,1 \exp(-5,3 P) \quad (\text{MPa}\sqrt{m})$$

$$\sigma_m = 392 \exp(-5,3 P) \quad (\text{MPa})$$

3.2. Unidirectional reinforced alumina

The presence of fibers impedes this shrinkage axially as well as radially. This is the typical problem of inhomogeneous sintering, and several authors (9,10) have proposed models. Presently, they deal only with particles and are at variance with experiment when the volume fraction is below 0.15. Nevertheless, they have shown that the presence of a reinforcement can considerably modify the final density of the matrix.

This has been verified in the present work for unidirectional alumina-FP and SiC-Nicalon fibers reinforced alumina. Table 6 gives the evolution of the matrix density (ρ_m), the porosity (Pm), the volume fraction of fibers (Vf) and the composite density (ρ_c) as a function of the sintering temperature (maintained 30 mn) for the two systems. Density and porosity of unreinforced alumina are recalled.

Sintering T° (*)	FP/alumina				SiC/alumina				Alumina alone	
	Vf	ρ_c	ρ_m	Pm	Vf	ρ_c	ρ_m	Pm	ρ_m	Pm
Green	0.37	2.72	1.99	0.50	0.230	2.30	2.27	0.42	2.39	0.40
1050°C	0.38	2.75	2.02	0.49	0.232	2.44	2.35	0.41	2.42	0.39
1150°C	0.40	2.81	2.05	0.48	0.236	2.51	2.46	0.38	2.65	0.33
1250°C	0.41	3.01	<u>2.34</u>	<u>0.41</u>	0.240	2.60	<u>2.56</u>	<u>0.35</u>	<u>3.22</u>	<u>0.19</u>

Table 6 - Sintering evolution of the matrix in uni-directional FP and SiC/alumina composites

(*) The highest sintering temperature of reinforced systems corresponds to the maximum thermal stability of the used SiC Nicalon fibers (NLM 202).

The comparison of the matrix porosities and densities at 1250°C between reinforced and unreinforced specimens (underlined numbers in table 6) emphasizes the drop in the sintering rate, mainly caused by the unrelaxed matrix shear stresses in the fiber preforms. Extended sintering durations do not modify significantly this limitation. Consequently, this single process involves a large matrix porosity which is not necessarily detrimental to the mechanical behaviour of large fiber volume reinforced ceramic composite (11).

The second aspect of this impeded sintering concerns the microcracks growth inside the matrix which could be caused by too high tensile stresses at the fiber-matrix interface during the sintering and the cooling steps. This investigation showed that such microcracks (radial and longitudinal) are not initiated in unidirectional composites when the temperature rate is low enough ($\sim 300^\circ\text{C}/\text{h}$) and essentially when the difference between fiber and matrix thermal expansion coefficients ($\Delta\alpha$) is positive or zero. Surfaces perpendicular and parallel to the fiber axis did not contain any microcrack in the alumina FP/alumina system sintered at 1250°C (temperature rate : 120°C/h ; upper sintering temperature maintained 30 mn) (Fig. 3), for which $\Delta\alpha = 0$. On the other hand, intense microcracking perpendicular to the fiber axis appear clearly in the SiC Nicalon/alumina system sintered in the same conditions (Fig. 4), for which $\Delta\alpha = -5,7 \cdot 10^{-6} \text{ } ^\circ\text{C}^{-1}$.

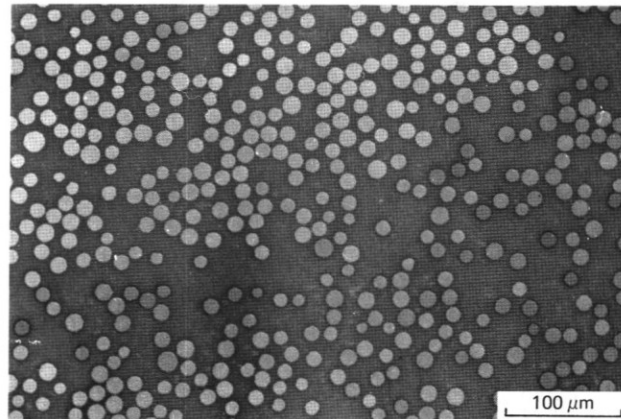


Figure 3. Optical micrograph of surface perpendicular to fiber axis showing the uncracked matrix of alumina FP/alumina composite sintered at 1250°C

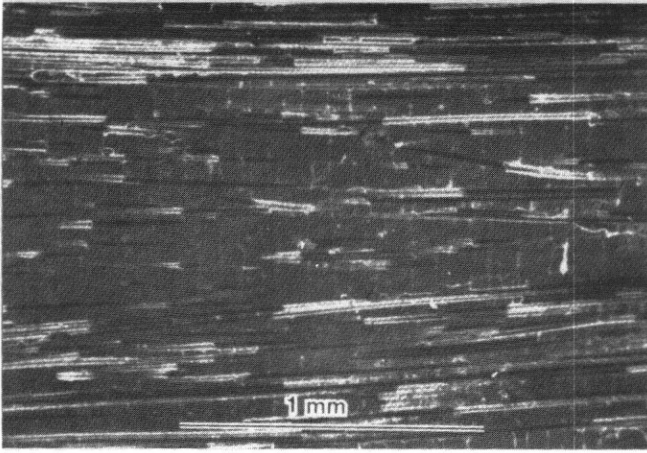


Figure 4. Scanning electron micrograph of a surface parallel to the fiber axis showing the regularly spaced array of microcracks in the matrix of a SiC Nicalon/alumina composite sintered at 1250°C

T.W. Coyle and al. (12) have shown that these microcracks spread out during cooling at a temperature (close to room temperature) which is directly connected to the longitudinal thermal stress :

$$\sigma_m^{th} = \frac{E_m E_f V_f}{E_c} (\Delta T \Delta \alpha)$$

Microcrack spacing distribution allowed also, through the ACK model and Vickers indentation technique, to determine a consistent value of the interfacial sliding frictional stress in this system. The value (50 MPa) is high, and it is not the result of an interface binding (Fig. 5) but can be explained by the tensile hoop stress at the interface generated during cooling.

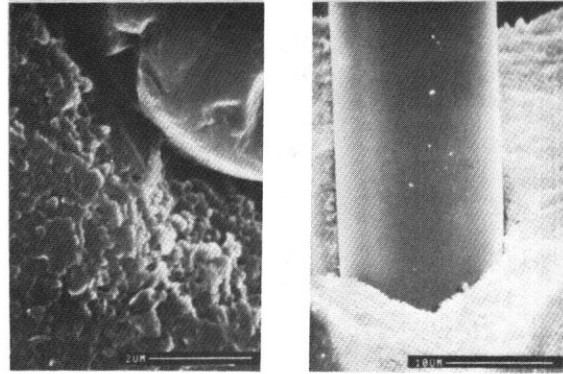
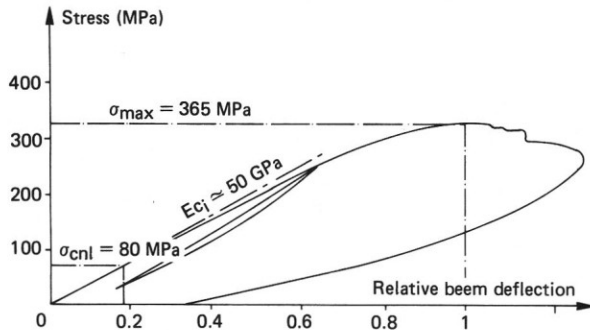


Figure 5. Micrographs of the SiC Nicalon/alumina interface showing the absence of binding and the smooth surface of the SiC fiber after process

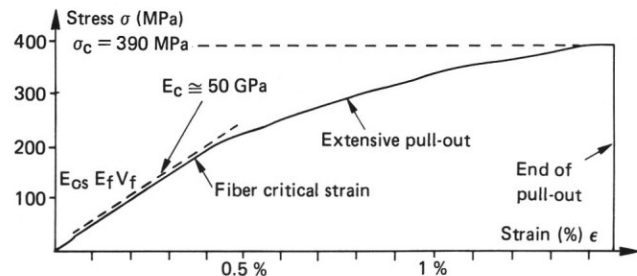
Finally, the mechanical behaviours of the two systems (12,13) are extremely different. The FP/alumina composite becomes very brittle when the sintering temperature increases and is an interesting system. On the other hand, the SiC Nicalon/alumina composite is significantly improved by sintering in spite of microcracks growth. Under flexural test, this composite sintered at 1250°C is able to support a maximum stress of 365 MPa with only 24 % fiber volume content and its toughness is considerably high (Fig. 6a). The stress-strain diagram under tensile stress of the same composite emphasizes the fiber critical and extensive pull-out strains. The ultimate strain can be up to 1.4 %, corresponding to a stress of 390 MPa when the fiber fracture starts approximately at 0.4 % (Fig. 6b).

3.3. 2D and 3D SiC Nicalon/alumina composites

After sintering (1250°C maintained 30 mn), dimensions and weight modifications of the green 2D and 3D composites described in table 4 are not significant. This involves a second mechanism of the microcracks growth connected to the matrix shrinkage and not only to the difference between the expansion coefficients of the components as in 1D composites.



(a) Flexure test



(b) Tensile test

Figure 6. Flexure and tensile stress/strain diagrams of the 1D-SiC/alumina composite ($V_f = 24\%$, sintering temperature = 1250°C)

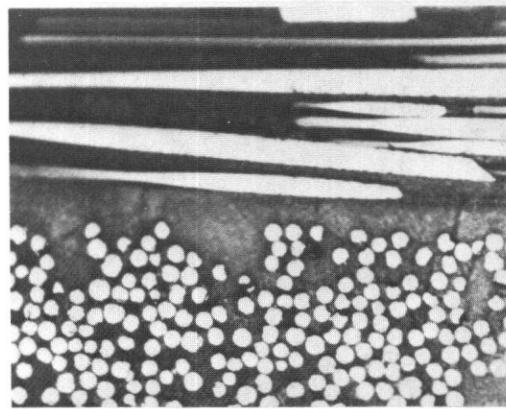
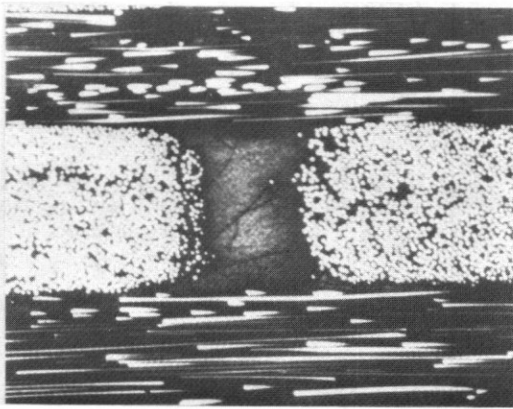


Figure 7. Microcrack networks in the 3D SiC Nicalon/alumina composite ($V_f = 0.44$ - sintering temperature = 1250°C)

The microscopic analysis of the microcracks network in the 3D composite (Fig. 7) showed :

- a evenly spaced system of microcracks oriented perpendicular to the fiber axis over the entire surface of tows parallel to the micrograph plane, like in the 1D composite ;
- no microcrack oriented radially to the fibers over the surfaces of tows perpendicular to the micrograph plane in which the fiber volume content is extremely high (up to 60 %) ;
- many randomly oriented microcracks in the unreinforced area included between the three orthogonal tows ;
- no connection between these two kinds of microcracks seems to be established.

Three points mechanical flexural tests have been operated on these composites with various sample sizes. The stress/deflection diagram of the 2D composite (Fig. 8) obtained with only two fabric plies shows a relatively low initial Young modulus (28 GPa) which is explained by the plain weaving. Besides, the maximum strength is up to 130 MPa and the relatively high residual strengths are maintained for very large deflections.

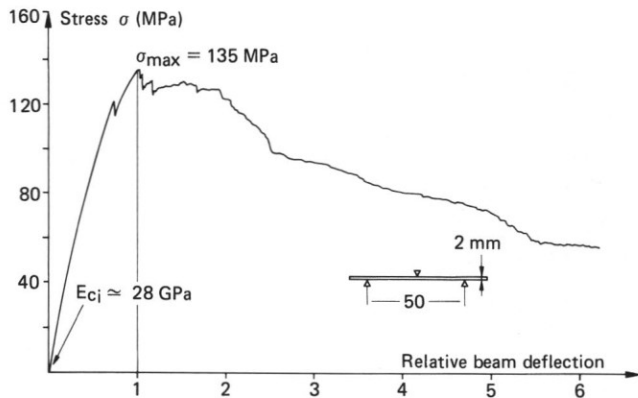


Figure 8. Three point flexure stress/deflection diagram of a 2D SiC Nicalon/alumina composite ($V_f = 0.3T$ - sintering temperature = 1250°C)

The stress/deflection diagram of 3D SiC Nicalon/alumina composite (Fig. 9) showed a relatively large initial Young modulus (98 MPa) which is explained by the participation of the matrix stiffness on the compression side of the thick sample (8 mm). The low span to thickness ratio (6.25) explained also the large stress range (200 MPa) over which the behaviour remains elastic. Besides, this test which induces a very large interlaminar shear stress, gives a maximum strength of 250 MPa when the sample sustains a relatively large deflection with an important toughness.

The macro fractography of the sample (Fig. 10) shows the absence of delamination and the extended tensile zone where the fibers failed.

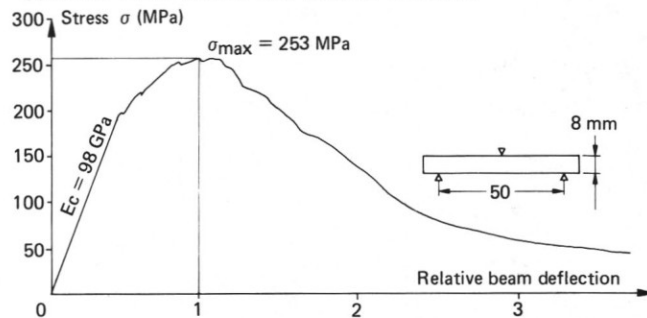


Figure 9. Three point flexure stress/deflection diagram of the 3D SiC Nicalon/alumina composite ($V_f = 0.44$ - sintering temperature = 1250°C)

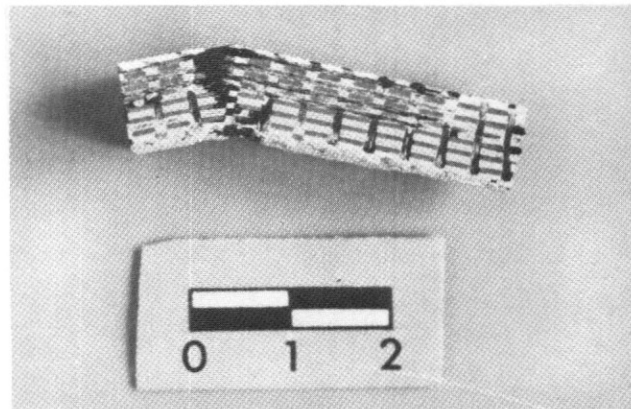


Figure 10. Macro-fractography of the 3D composite after flexure test

3 - CONCLUSION

The high yield infiltration of ceramic colloidal particles in dense and thick multi-D fiber preforms using the pressure slip casting technique has been demonstrated on practical systems. The effectiveness of the process is illustrated by a direct and homogeneous deposition of α -alumina powder (mean size : 0.3 μ m) into a thick 3D SiC Nicalon fiber preform (thickness : 8 mm ; volume fiber content : 45 %) with a green density close to 2300 kg/m³. This green matrix density is 95 % of those obtained without preform. The extension of such a process to various powders (SiC - Si₃N₄ - ZrO₂ - etc...) completed by other liquid densification methods (polymer precursors and sol-gel) opens a promising route to the ceramic composites development.

The investigation of the alumina matrix free sintering into 1D fiber preforms showed that :

- shrinkage is strongly impeded by the fibers ;
- microcrack formation is avoided by diffusion controlled creep if the difference between fiber and matrix expansion coefficients is at least zero.

In spite of matrix porosity and microcracking, large strengths (1D - 350 MPa, 3D - 250 MPa) and ultimate elongations ($\epsilon >$ 1.4 %) are obtained in the SiC Nicalon/alumina composites sintered at 1250°C ; this result is mainly explained by an unbound fiber-matrix interface.

REFERENCES

- 1 - J. Jamet, J.R. Spann, R.W. Rice, D. Lewis and W.S. Coblenz
"Ceramic-fiber composite processing via polymer filler matrices"
Ceram. Eng. Sci. Proc. 5 (7-8) 677-694 (1984)
- 2 - L. Svarovsky
"Solid-liquid separation"
Butterworths, London (1981)
- 3 - I.A. Aksay, F.F. Lange, B.I. Davis
"Uniformity of Al₂O₃-ZrO₂ composites by colloidal filtration"
J. Am. Cer. Soc. 66 (10) C-190-C-192 (1983)
- 4 - I.A. Aksay
"Colloidal filtration route to uniform composite microstructure"
Proceeding of Inter. Conf. on Ultrastructure Processing of Ceramics, Glasses and Composites Feb. 13-17 (1983) Gainesville, Florida
- 5 - I.A. Aksay, F.F. Lange, B.I. Davis
"Mechanics of colloidal filtration"
pp. 85-93 in Advances in Ceramics Vol. IX, Forming of Ceramics, Am. Cer. Soc. Inc. Columbus Ohio (1981)
- 6 - J. Gregory
"Flocculation and Filtration of Colloidal Particles"
Proceeding of Int. Conf. on Ultrastructure Processing of Ceramics, Glasses and Composites Gainesville, Florida (Feb. 13-17 (1983)
- 7 - L.A. Spielman
Ann. Rev. Fluid Mech. 9 297 (1977)
- 8 - K. Yao, M.T. Habobion, C.R. O'Melia
Env. Sci. Technol. 5, 1105 (1971)
- 9 - R. Raj, R.K. Bordia
"Sintering Behaviour of Bimodal Powder Compacts"
Acta Metall. 32 (7) 1003-19 (1984)
- 10 - R.K. Bordia, R. Raj
"Analysis of Sintering of a Composite with Glass or Ceramic Matrix"
J. Am. Cer. Soc. 69 (3) C-55-C-57 (1986)
- 11 - J. Jamet, M.H. Guyot, D. Abbé
ONERA T.R. n° 11/3548 M 3 (1984)
- 12 - T.W. Coyle, M.H. Guyot, J.F. Jamet
"Mechanical Behaviour of Microcracked Ceramic Composite"
To be published in Proceedings of the 10th Annual Conf. on Composites and Advanced Ceramics Cocoa Beach, Florida (Jan. 1986)
- 13 - J.F. Jamet, D. Abbé, M.H. Guyot
"Interface and Matrix Optimization in Sintered Ceramic Composites"
ICCM V, San Diego, July 30 (1985)